

## Supplementary Materials

### Influence of Process Parameters on the Microstructural Properties of Spray-Pyrolyzed $\beta\text{-Ga}_2\text{O}_3$

Constance Schmidt, Axel Fechner, Oleksandr Selyshchev, and Dietrich R. T. Zahn

Semiconductor Physics, Chemnitz University of Technology, D-09107 Chemnitz, Germany

\*Correspondence: [oleksandr.selyshchev@physik.tu-chemnitz.de](mailto:oleksandr.selyshchev@physik.tu-chemnitz.de), [zahn@physik.tu-chemnitz.de](mailto:zahn@physik.tu-chemnitz.de)

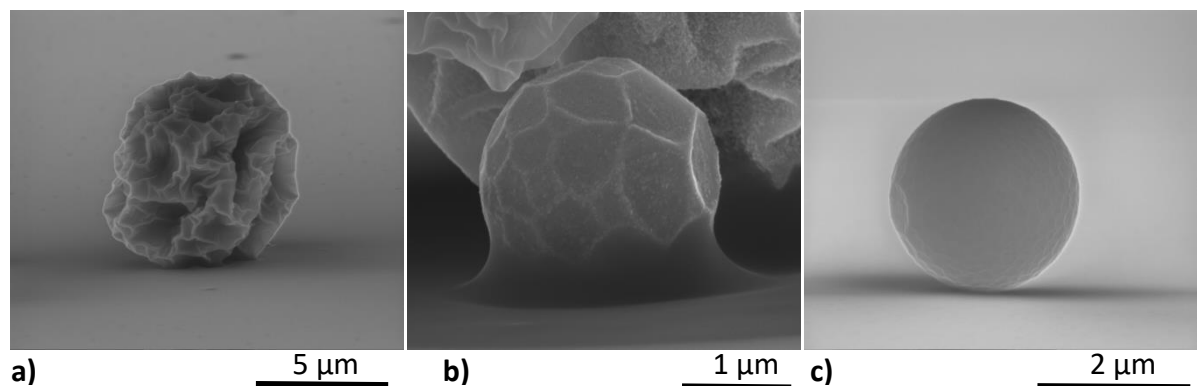


**Figure S1.** SEM images of differently shaped  $\beta\text{-Ga}_2\text{O}_3$  spheres: a) by adding tenside solution; b) without any additions; and c) with adding ethanol to the solution.

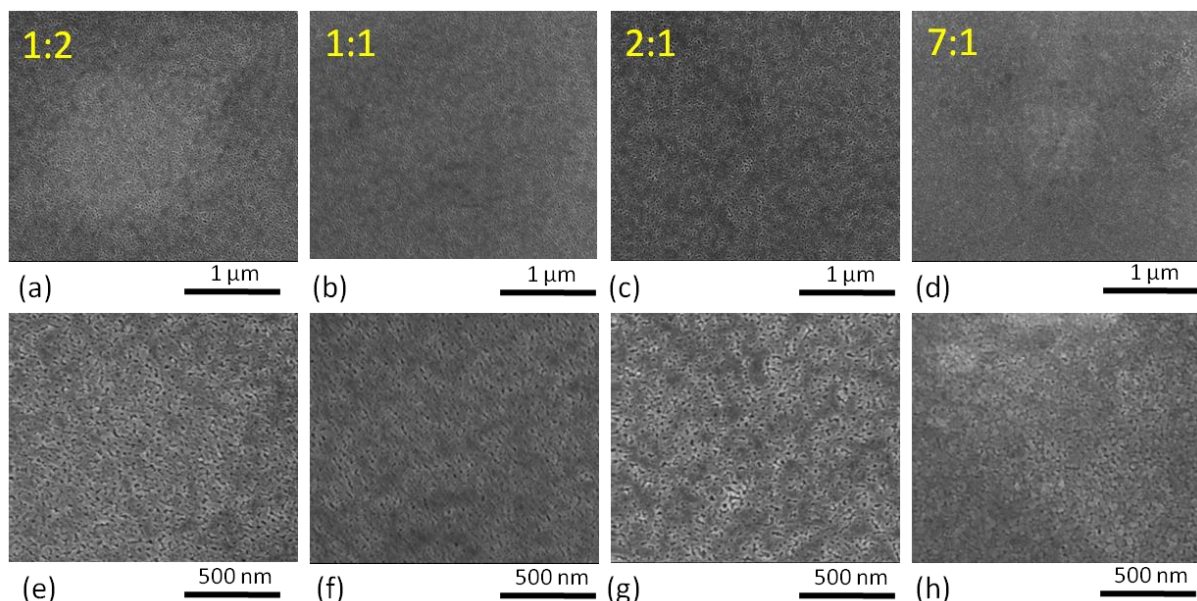


**Figure S2.** SEM images of  $\beta\text{-Ga}_2\text{O}_3$  thin films prepared with different EtOH to water ratios: (a) and (e) 1:2, (b) and (f) 1:1, (c) and (g) 2:1, (d) and (h) 7:1.

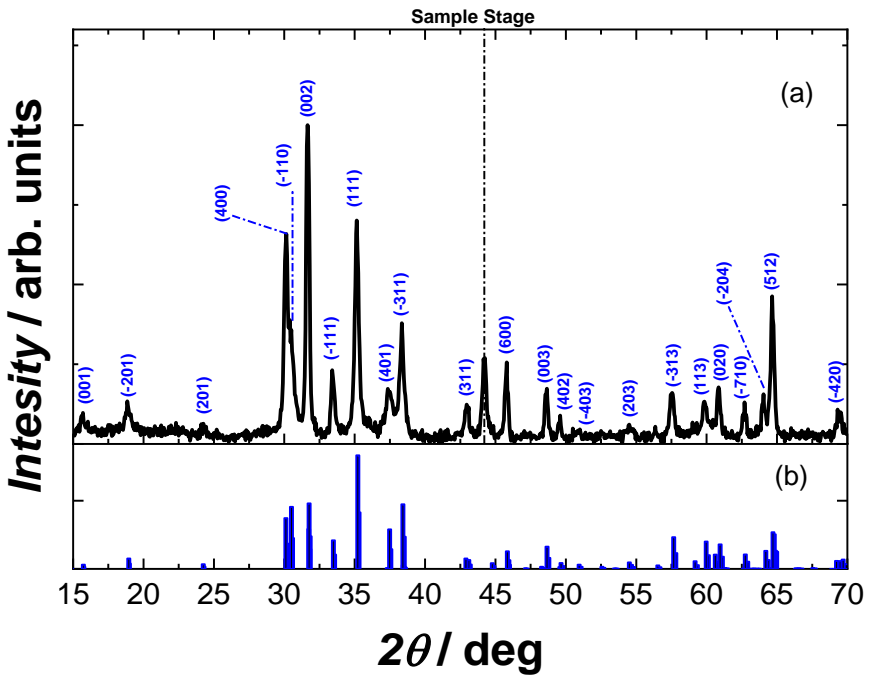


**Figure S3.** a) Indexing of the XRD pattern. Sample - flake microstructures. Assignment to  $\beta$ -Ga<sub>2</sub>O<sub>3</sub> according to the ICSD card #83645; b) XRD pattern simulated using VESTA software (ref. [63] in the main text) and  $\beta$ -Ga<sub>2</sub>O<sub>3</sub> crystal structure from the Crystallography Open Database (COD), card number #2004987.

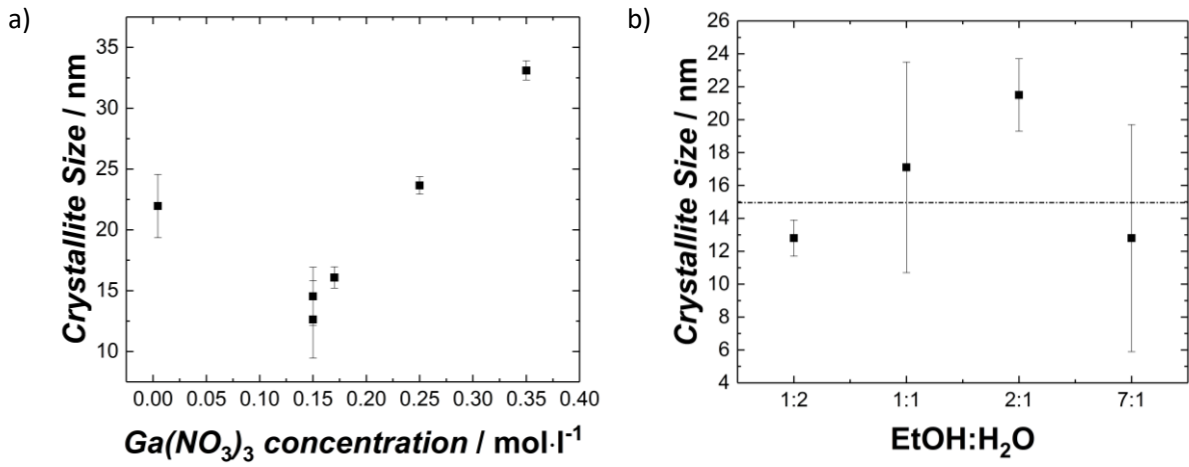


**Figure S4.** a) Calculated crystallite size for  $\beta$ -Ga<sub>2</sub>O<sub>3</sub> microstructures in dependence of the Ga(NO<sub>3</sub>)<sub>3</sub> concentration; b) Calculated crystallite size for  $\beta$ -Ga<sub>2</sub>O<sub>3</sub> thin films obtained with different EtOH:H<sub>2</sub>O ratios.

**Table S1.** Explanation for the origin of the Raman modes. Mode position is taken from the Raman modes of the thin  $\beta$ - $\text{Ga}_2\text{O}_3$  films. Notation of the atoms is adopted from refs [41,57] cited in the main text.

Mode position	Symmetry	Example of corresponding atoms
200.3	$A_g$	Libration and translation of chains
319.8	$A_g$	Torsion around $\text{Ga}_1\text{-O}_7$ axis
342.9	$A_g$	Bending of $\text{O}_{11}\text{-Ga}_1\text{-O}_9$ & $\text{O}_5\text{-Ga}_1\text{-O}_7$
349.7	$B_g$	Bending of $\text{O}_5\text{-Ga}_1\text{-O}_9$
415.9	$A_g$	Bending of $\text{O}_5\text{-Ga}_1\text{-O}_7$ & Stretching of $\text{O}_{11}\text{-Ga}_1\text{-O}_9$
475.0	$A_g$	Bending of $\text{O}_{13}\text{-Ga}_3\text{-O}_{11}$ & Stretching of $\text{Ga}_1\text{-O}_5$
628.3	$A_g$	Stretching of $\text{Ga}_3\text{-O}_9$
651.6	$B_g$	Stretching of $\text{Ga}_1\text{-O}_7$
658.6	$A_g$	Stretching of $\text{Ga}_3\text{-O}_{13}$ & Bending of $\text{O}_{13}\text{-Ga}_3\text{-O}_{11}$
765.6	$A_g$	Stretching of $\text{Ga}_1\text{-O}_5$ & $\text{Ga}_3\text{-O}_{13}$

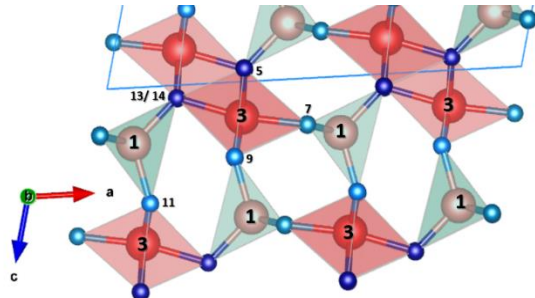


**Figure S5.** Sketch of the crystal lattice of  $\beta$ - $\text{Ga}_2\text{O}_3$  (created with VESTA software, ref. [63] in the main text) with indication of Ga and O atoms for the explanation of the origin of the Raman modes.

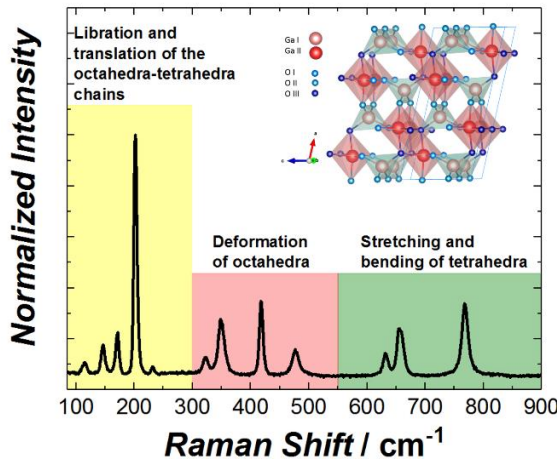


**Figure S6.** Raman spectrum of bulk like  $\beta$ - $\text{Ga}_2\text{O}_3$  on quartz glass taken with an excitation of 514.7 nm separated in the three parts of the spectrum.

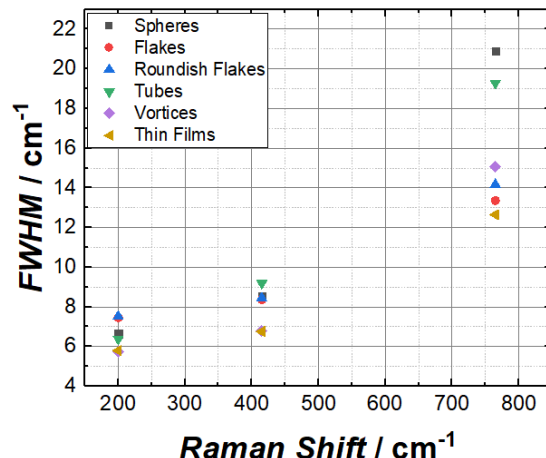


**Figure S7.** FWHM of the Raman modes for different  $\beta$ - $\text{Ga}_2\text{O}_3$  microstructures. For every part of the Raman spectrum of  $\beta$ - $\text{Ga}_2\text{O}_3$  we chose one mode ( $200 \text{ cm}^{-1}$ ,  $415 \text{ cm}^{-1}$ , and  $765 \text{ cm}^{-1}$ ).

**Table S2.** Stress and Raman shifts for the different microstructures.

Microstructure	Stress / GPa	Experimental Raman shift / $\pm 0.6 \text{ cm}^{-1}$	Experimental Raman shift / $\pm 0.6 \text{ cm}^{-1}$	Experimental Raman shift / $\pm 0.6 \text{ cm}^{-1}$
Flakes	$-1.68 \pm 0.31$	199.3	415.3	764.9
Round flakes	$-3.15 \pm 0.63$	200.1	416.0	766.0
Tubes	$1.68 \pm 0.52$	199.2	414.9	759.6
Vortices	$2.00 \pm 0.31$	200.2	415.9	765.5
Spheres	$-5.98 \pm 0.31$	199.7	415.6	763.5

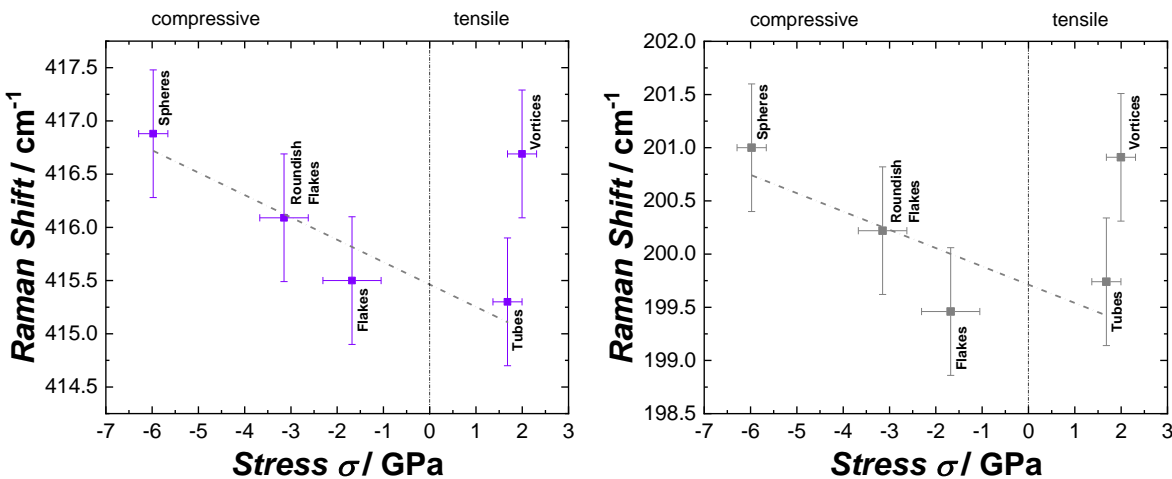


**Figure S8.** Raman shifts of all microstructures in dependence of the measured stress: a) mode around  $200 \text{ cm}^{-1}$ , b) mode around  $415 \text{ cm}^{-1}$ . In every case a negative slope from compressive to tensile stress is visible. The dashed line is a guide for the eye. Only vortices do not fit to the observed trend.

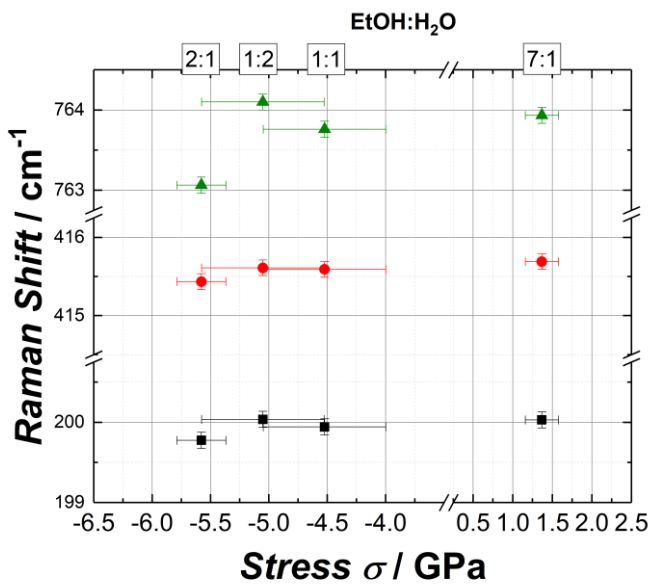


**Figure S9.** Raman shifts of thin films prepared at different EtOH:H<sub>2</sub>O ratios in dependence of the measured stress for the modes around  $200 \text{ cm}^{-1}$ ,  $415 \text{ cm}^{-1}$ , and  $765 \text{ cm}^{-1}$ . While the Raman shift is almost constant, the stress changes from compressive to tensile by adding more ethanol to the solution.

#### References (the same references are cited in the main text):

41. Schmidt, C.; Rahaman, M.; Zahn, D.R.T. Conversion of 2-dimensional GaSe to 2-dimensional  $\beta$ -Ga<sub>2</sub>O<sub>3</sub> by thermal oxidation. *Nanotechnology* **2022**, *33*, 045702. <https://doi.org/10.1088/1361-6528/ac2f5d>.
57. Dohy, D.; Lucaleau, G.; Revcolevschi, A. Raman spectra and valence force field of single-crystalline  $\beta$ -Ga<sub>2</sub>O<sub>3</sub>. *J. Solid State Chem.* **1982**, *45*, 180–192. [https://doi.org/10.1016/0022-4596\(82\)90274-2](https://doi.org/10.1016/0022-4596(82)90274-2).
63. Momma, K.; Izumi, F. VESTA 3 for three-dimensional visualization of crystal, volumetric and morphology data. *J. Appl. Crystallogr.* **2011**, *44*, 1272–1276. <https://doi.org/10.1107/S0021889811038970>.